Available online at www.sciencedirect.com
ScienceDirect
International Journal of Heat and Mass Transfer 50 (2007) 1221–1230
International Journal of HEAT and MASS TRANSFER
www.elsevier.com/locate/ijhmt

A novel method to increase the growth rate in sublimation crystal growth of advanced materials

Xiaolin Wang *, Dang Cai, Hui Zhang

Department of Mechanical Engineering, State University of New York at Stony Brook, Stony Brook, NY 11794, USA

Received 9 July 2006; received in revised form 16 September 2006
Available online 29 November 2006

Abstract

Sublimation crystal growth technique is widely used for the growth of optoelectronic materials, such as aluminum nitride (AlN). In this paper, an integrated model is developed to study the effects of powder geometry on crystal growth rate whereas induction heating, powder charge sublimation, vapor transport, and porosity evolution are considered. The mechanism of vapor transport is proposed by introducing a driving force arising from the temperature difference in AlN sublimation growth system. Powder porosity evolution and sublimation rate variation are predicted based on the vapor transport mechanism. In addition, a new method by optimizing the initial powder porosity and creating holes in the packed powder is proposed to increase the crystal growth rate. Simulation results for the sublimation of powder with and without central hole are presented. It is found that the powder sublimation rate is higher when hole is present. This is also validated experimentally. Effects of initial porosity, particle size and driving force on the sublimation rate are also studied. Finally, the powder geometry is optimized based on numerical simulations. The findings from this investigation can also be applied to SiC since SiC sublimation growth is similar to AlN.

Keywords: Sublimation; Powder; Crystal; Growth; Rate; Porosity

1. Introduction

Group III nitrides (AlN, GaN, InN) are wide band-gap materials with superior physical and electronic properties for blue/UV lasers, optical sources and detectors, and high-power and high temperature devices [1–4]. AlN is a promising candidate for electronic, optical and opto-electronic applications due to its high thermal conductivity, high electrical resistivity, high acoustic wave velocity and large band gap [1–3]. It can be used in producing blue-emitting LEDs and second harmonic generators for its highly non-linear optical susceptibilities [5].

Sublimation technique is recognized as the most promising method to produce large bulk AlN single crystals at present [1,6–9]. In a sublimation system, AlN crystals are produced from AlN source at a temperature above 1800 °C in a nitrogen environment. Sublimation growth process consists of following steps: sublimation of source material, transport in the gas phase, impingement of atoms at the seed surface, surface diffusion, and surface adsorption or desorption [10].

In the past decades, many research groups have worked on the growth of AlN bulk crystals to increase crystal growth rate. Traditional approaches for enhancing the growth rate are to increase furnace temperature or change pressure. High cost of inert crucible that can sustain high temperature and impurity caused by crucible degradation set limit on the maximum growth rate. Presence of certain chemical species in the crucible material can alter the crystal growth habit by changing the fastest growth direction. Incorporation of impurities from crucible can also generate stresses and defects in the crystal. Moreover, existence of

* Corresponding author. Tel.: +1 631 632 8303; fax: +1 631 632 8544.
E-mail address: xiaolinw@ic.sunysb.edu (X. Wang).

0017-9310/$ - see front matter © 2006 Elsevier Ltd. All rights reserved.
doi:10.1016/j.ijheatmasstransfer.2006.09.021

Nomenclature

A_0	magnetic vector potential (Wb/m)
A_r	in-phase component, real part (Wb/m)
A_i	out-phase component, imaginary part (Wb/m)
c_p	isobaric specific heat (J/kg K)
d_p	average particle diameter of AlN powder (m)
$F_{j,k}$	view factor
ΔG	free energy (J/mol)
H	height of the crucible (m)
ΔH	enthalpy (J/mol)
J_0	current density (A/m^2)
k	thermal conductivity (W/m K)
K	permeability (m^2)
K_p	equilibrium constant
L_d	distance between source and side (m)
l_{th}	reaction zone thickness (m)
q'	radiative heat flux (W/m^2)
P	pressure (Pa)
r	radial coordinate
R	universal gas constant, 8.314 (J/mol K)
$\dot{R}$	reaction rate
ΔS	entropy (J/mol K)
t	time (s)
T	temperature (K)
ΔT	temperature difference between source and seed (K)
u	velocity vector
z	axial coordinate
Z	pre-exponential in Eq. (25)
Z_{th}	constant in Eq. (28)

Greek symbols

σ	Stefan–Boltzmann constant (W/m^2 K^4)
σ_c	electrical conductivity (1/Ω m)
ε	emissivity
ε_m	permittivity (F/m)
ε_p	porosity
μ	viscosity (kg/m s)
μ_m	magnetic permeability (H/m)
v	kinematic viscosity, μ/ρ (m^2/s)
ρ	density (kg/m^3)
ω	angular frequency of the AC current (rad/s)

Subscripts

Al	aluminum
AlN	aluminum nitride
df	driving force
e	equilibrium
eddy	eddy current
eff	effective
latent	latent heat related parameter
N_2	nitrogen
r	radial
radi	radiative
s	source
seed	seed
solid	solid
s,side	side surface of source
s,top	top surface of source
total	total

Superscripts

s	source
seed	seed
s,side	side surface of source
s,top	top surface of source

crucible and other components in the furnace is no longer passive at high temperatures as their gas pressure may be significant, or they may react with the source material (AlN powder) and nitrogen.

Geometry and properties of the powder source are believed to affect the sublimation growth significantly as a whole. Little has been known so far to the mechanisms of species transport inside the powder because the sublimation growth is operated at an extremely high temperature in a closed enclosure. This prevents in situ monitoring and measurement of key process parameters which are necessary for understanding the growth process. To determine optimal growth conditions for large diameter crystal with high quality and growth rate, it is important to thoroughly understand the interplay between vapor transport and powder sublimation, in particular powder porosity evolution and gas transport during powder sublimation.

This paper will present comprehensive studies of powder geometric effects on the sublimation rate. A physics-based computational model will be developed considering powder sublimation and porosity evolution. Based on the proposed model, the effect of a central hole in the powder on the sublimation rate is studied and the result is compared to the case of powder without a hole. The effects of initial porosity, particle size and driving force on the sublimation rate are also studied. Optimal powder geometry is proposed based on numerical simulations.

2. System description

Fig. 1a shows an AlN sublimation growth system being studied here. AlN growth is driven by temperature difference $\Delta T = T_s - T_{seed}$ between the AlN powder material source (T_s) and single crystal AlN seed (T_{seed}). The growth cell contains a substrate with seed and AlN powder as the source material separated by a stream of nitrogen gas. It is placed into a special crucible with a temperature gradient zone where the growth of AlN crystal is initiated. The sub-

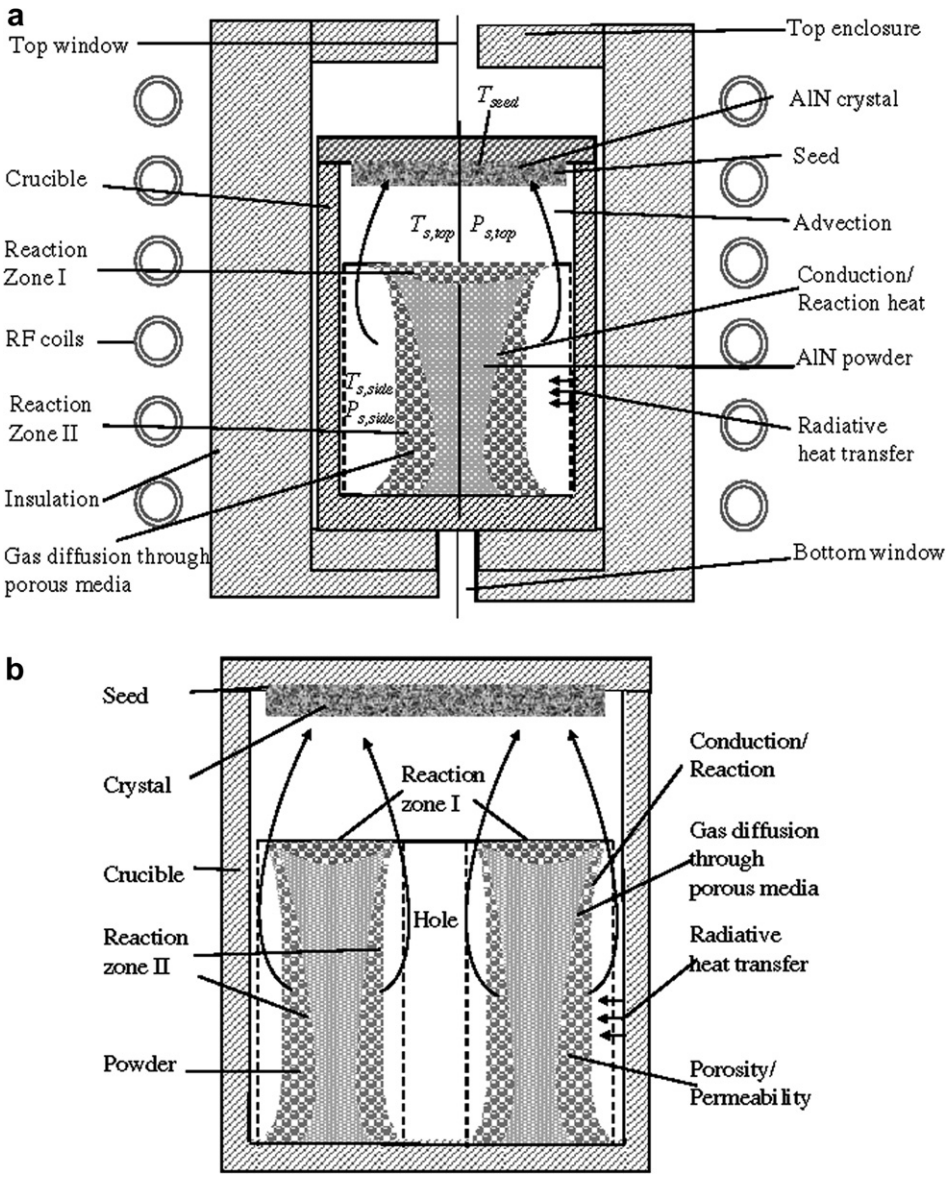

Fig. 1. Schematic of powder sublimation and porosity evolution in a sublimation crystal growth system: (a) no hole and (b) a central hole is created.

strate temperature is maintained at 1800–2300 °C during growth. The temperature difference between the source and substrate varies within 30–90 °C. It is noted that the side surface of powder is sublimed first as the result of relatively higher temperature at the lower portion of crucible. The gas phase in the crucible is constituted by two major species, i.e. aluminum vapor (Al) and nitrogen gas (N_2). These two species only react with each other on the source and seed surfaces. The species fluxes are directed from the source to the seed. Depending on temperature differences between the seed, top and side surfaces of powder charge, the top surface of the powder may sublime to produce vapor species for crystal growth; may be deposited by vapor species, subsequently retard growth at the seed. The growth process is usually carried out in a nitrogen environment at 50–760 Torr [11].

3. Scale analysis

To provide basic understanding of the complex vapor transport phenomena in AlN growth system, and determine control properties for vapor transport in AlN powder, the importance of dimensionless parameters, e.g., Darcy and Reynolds numbers in the system is analyzed. To quantify the gas transport in the porous material, the Darcy number is defined as

$$Da = \frac{\Delta P \cdot 2D_0}{\rho u^2 L} \tag{1}$$

where ΔP is the pressure drop, D the diameter, ρ the fluid density, u the fluid velocity, and L the length over which the pressure drop is measured. Using $\Delta P = 100$ Pa, $u = 0.2$ m/s from simulation based on Eqs. (13) and (16),

and $D_0 = 1 \times 10^{-5}$ m, $\rho = 0.1502$ kg/m^3, and $L = 1.9 \times 10^{-2}$ m, the Darcy number is estimated as 175, indicating that vapor produced can escape the porous media with the given pressure gradient.

To quantify the flow intensity, the value of the Reynolds number is estimated from

$$Re = \frac{\rho u L}{\mu} \tag{2}$$

where μ is dynamic viscosity. Using $\mu = 6.426 \times 10^{-5}$ kg/m s and $u = 2 \times 10^{-1}$ m/s, the Reynolds number is calculated as 9.0, indicating the gas transport in porous media follows laminar flow behavior and the viscous force dominates the flow.

It is common understanding that chemical reactions, both exothermic and endothermic, will not contribute significantly to heat transfer and temperature distribution in the AlN growth system [11]. This assumption will also be used in this study.

4. Induction heating system model

In the AlN growth, an induction heating is used. To estimate the heating power to the growth unit, the electromagnetic field and the Joule heat produced by induction heating coils are calculated by the Maxwell equations, and the heat flux to the growth unit is obtained from temperature distribution for the entire growth system by solving the energy equation accounting for conduction and radiation within and between various components.

For a frequency lower than 1 MHz, the electromagnetic field can be assumed as quasi-steady and axisymmetric, and the current in the coil is time harmonic. The Joule heat is generated solely by the eddy current in the crucible. The azimuthal component A_0 ($A_0 = A_r + iA_i$) of the magnetic vector potential is solved for induction heating coils. The Maxwell equations in terms of A_r and A_i can be written as follows [12,13]:

$$\left[\frac{\partial^2}{\partial r^2} + \frac{1}{r}\frac{\partial}{\partial r} - \frac{1}{r^2} + \frac{\partial^2}{\partial z^2}\right]\left[\frac{A_r}{\mu_m}\right] + \varepsilon_m \omega^2 A_r + \omega \sigma_c A_i = -J_0 \tag{3}$$

$$\left[\frac{\partial^2}{\partial r^2} + \frac{1}{r}\frac{\partial}{\partial r} - \frac{1}{r^2} + \frac{\partial^2}{\partial z^2}\right]\left[\frac{A_i}{\mu_m}\right] + \varepsilon_m \omega^2 A_i - \omega \sigma_c A_r = 0 \tag{4}$$

where the real part, A_r, and the imaginary part, A_i, are referred as the in-phase and out-of-phase components, respectively, and J_0 is the current density in the azimuthal direction in induction heating coils. The heat generated by the eddy current in the graphite susceptor can be expressed as $q''_{eddy} = \frac{1}{2}\sigma_c \omega^2 (A_r^2 + A_i^2)$.

It is assumed that the contribution of convective heat transfer inside the gas phase is negligible. The energy transport equation can be written as follows:

$$(\rho c_p)_{eff} \frac{\partial T}{\partial t} = \nabla \cdot (k_{eff} \nabla T) + q'''_{eddy} + q'''_{latent} + \nabla \cdot q''_{radi} \tag{5}$$

where q''_{radi} represents the radiative heat flux on the surfaces of inner enclosure. For sublimation growth, the source material is porous media. The effective heat capacity $(\rho c_p)_{eff}$ and thermal conductivity k_{eff} can be estimated from

$$(\rho c_p)_{eff} = \varepsilon_p (\rho c_p)_{gas} + (1 - \varepsilon_p)(\rho c_p)_{solid} \tag{6}$$

$$k_{eff} = \varepsilon_p \left(k_{gas} + \frac{32}{3}\varepsilon \sigma T^3 d_p\right) + (1 - \varepsilon_p) k_{solid} \tag{7}$$

where $0 \leqslant \varepsilon_p < 1$ is the porosity of AlN powder (the void fraction of gas in the powder) and d_p is the average particle diameter of the powder. k_{gas} and k_{solid} are thermal conductivities of gas and solid, respectively.

In the crucible, gas and gas species can be considered as transparent, and all the surfaces are gray and diffusive. The grid-to-grid gray-diffusive method requires the faces in the computational domain being divided into grids. The radiation surfaces are thus divided into a number of rings, each with uniform properties. The rings coincide with the grids defined in the curvilinear finite volume method, and the view factors between each pair of rings are calculated. The total exchange factor method, one of the zonal methods, has been used to relate the temperature at the grid with the heat flux q''_{radi} [14], while q''_{radi} is calculated by solving the following radiation equation for gray and diffusive surfaces:

$$\frac{q''_{radi,j}}{\varepsilon_j} - \sum_{k=1}^{N} F_{j,k} \frac{1 - \varepsilon_k}{\varepsilon_k} q''_{radi,k} = \sigma T_j^4 - \sum_{k=1}^{N} F_{j,k} \sigma T_k^4 \tag{8}$$

where $F_{j,k}$ is the view factor from ring j to k, and ε is the emissivity of radiative surface.

5. Powder sublimation and porosity evolution model

Key components in the growth system have been clearly depicted in Fig. 1a. The crucible is 3.8 cm in diameter (D) and 5.4 cm in height (H). The temperature of the seed is T_{seed}, and the temperatures of the side surface and top surface of the powder source are $T_{s,side}$ and $T_{s,top}$, respectively. T_{seed} is usually 30–90 °C lower than $T_{s,side}$ and $T_{s,top}$ to ensure the atoms produced by the powder sublimation being adsorpted or desorpted on the seed surface.

Sublimation of AlN can be represented by

$$\text{AlN (s)} \leftrightarrow \text{Al (g)} + 1/2\,\text{N}_2\text{ (g)} \tag{9}$$

Powder density is defined as the mass of the powder divided by the volume the mass occupies. This volume does not include the void volume of gas in the powder. Porosity is defined as the void fraction of gas in the porous media. The powder size distribution changes with process due to sintering, however, porous media model based on Darcy's law is unable to describe such distribution or change. Therefore, the particle size and void changes due to sintering during crystal growth are neglected in this paper. In addition, the following assumptions are made for the powder sublimation and porosity evolution model: (1) particles have uniform size, (2) powder density remains constant, (3)

gas and solid phases are in thermal equilibrium locally, and (4) radiation heat transfer within the powder can be incorporated into an effective thermal conductivity.

Based on the above assumptions, the mass conservation equation is simplified as follows:

$$\frac{\partial \rho_{\text{solid}}(1-\varepsilon_{\text{p}})}{\partial t} = -\dot{R} \tag{10}$$

where ρ_{solid} is the mass density of the solid (AlN), ε_{p} the powder porosity, and $\dot{R}$ the sublimation rate, i.e. the powder mass loss rate. According to assumption (2), the following equation can be derived from Eq. (10):

$$\frac{\partial \varepsilon_{\text{p}}}{\partial t} = \frac{\dot{R}}{\rho_{\text{solid}}} \tag{11}$$

The equation of continuity in the cylindrical coordinate is [15]

$$\frac{\partial}{\partial t}\left[\rho_{\text{solid}}(1-\varepsilon_{\text{p}}) + \rho_{\text{g}}\varepsilon_{\text{p}}\right] + \frac{1}{r}\frac{\partial}{\partial r}\left(r\varepsilon_{\text{p}}\rho_{\text{g}}u_r\right) + \frac{\partial}{\partial z}\left(\varepsilon_{\text{p}}\rho_{\text{g}}u_z\right) = 0 \tag{12}$$

where ρ_{g} is the mass density of gas N_2 and Al vapor, and u_r and u_z are radial and axial gas velocities, respectively.

Gas pressure in the powder can be derived from the Darcy's law:

$$\nabla P = \frac{\mu}{K}\vec{u} \tag{13}$$

where K is the local permeability of the powder and given by

$$K(\varepsilon_{\text{p}}) = \frac{d_{\text{p}}^2\varepsilon_{\text{p}}^3}{175(1-\varepsilon_{\text{p}})^2} \tag{14}$$

where d_{p} is the mean diameter of particles.

Reaction starts from both side and top surfaces of the powder, and two reaction zones (reaction zones I and II) are formed. It is assumed that vapor produced in reaction zone I escapes from the top surface of the powder with an axial velocity only, and the radial velocity u_r is negligible in Eq. (12). Therefore, for gases in reaction zone I, the momentum equation can be simplified as

$$P(r,z) = P_{\text{s,top}}(r) + \int \frac{\mu}{K(r,z)}u_z(r,z)\mathrm{d}z \tag{15}$$

where $P_{\text{s,top}}(r)$ is the gas pressure at the top surface of the powder. We define $\Delta P(r,z)$ as the pressure difference between the location (r,z) and reaction zone I:

$$\Delta P(r,z) = P(r,z) - P_{\text{s,top}}(r) \tag{16}$$

Similarly, it is assumed that vapor produced in reaction II escapes from the side surface of the powder with a radial velocity only. Therefore, for gases in reaction zone II, the momentum equation can be simplified as

$$P(r,z) = P_{\text{s,side}}(z) + \int \frac{\mu}{K(r,z)}u_r(r,z)\mathrm{d}r \tag{17}$$

where $P_{\text{s,side}}(z)$ is the gas pressure at the side surface of the powder and $\Delta P(r,z)$ is the pressure difference between the location (r,z) and reaction zone II:

$$\Delta P(r,z) = P(r,z) - P_{\text{s,side}}(z) \tag{18}$$

Powder sublimation is related to both powder temperature and vapor (Al vapor and N_2 gas) transport. Vapor can be transported from the powder source to the seed by the driving force arising from the temperature difference between the source and seed surfaces. For the sublimation growth, it is widely assumed that the total pressure inside the crucible is higher than that outside the crucible. Therefore, diffusion rate of nitrogen gas is low. Thus, the pressure of nitrogen gas at the seed and source surfaces is close to the stoichiometric partial pressure. Therefore, the driving force, designated by P_{df}, can be formulated by equilibrium total gas pressure difference between the source and seed surfaces. In reaction zones I and II, the driving forces are expressed as Eqs. (19) and (20), respectively:

$$P_{\text{df}} = P_{\text{e,total}}^{\text{s,side}} - P_{\text{e,total}}^{\text{seed}} \tag{19}$$

$$P_{\text{df}} = P_{\text{e,total}}^{\text{s,top}} - P_{\text{e,total}}^{\text{seed}} \tag{20}$$

where $P_{\text{e,total}}^{\text{s,side}}$ and $P_{\text{e,total}}^{\text{s,stop}}$ are the equilibrium total pressures on the side and top surfaces of the source, respectively. $P_{\text{e,total}}^{\text{seed}}$ is the equilibrium total pressure on the seed surface. The equilibrium total pressure satisfies:

$$P_{\text{e,total}} = P_{\text{e,Al}} + P_{\text{e,N}_2} \tag{21}$$

where $P_{\text{e,Al}}$ and $P_{\text{e,N}_2}$ are the equilibrium partial pressures of aluminum and nitrogen, respectively. According to sublimation reaction (9), the relationship between two partial pressures satisfies:

$$P_{\text{e,Al}} = 2P_{\text{e,N}_2} \tag{22}$$

From thermodynamics, two partial pressures satisfy:

$$\frac{P_{\text{e,Al}}}{P_{\text{a}}}\left(\frac{P_{\text{e,N}_2}}{P_{\text{a}}}\right)^{1/2} = K_{\text{p}} = \exp\left(-\frac{\Delta G}{RT}\right) = \exp\left(\frac{\Delta S}{R} - \frac{\Delta H}{RT}\right) = \exp\left(A - \frac{B}{T}\right) \tag{23}$$

where ΔS, ΔH and ΔG are the entropy, enthalpy and Gibbs free energy of sublimation, respectively. Using published data $\Delta H = 630.1$ kJ/mol and $\Delta S = 224.9$ J/mol K [1,16], constants A and B in Eq. (23) can be calculated as

$$A = \frac{\Delta S}{R} = 27.055 \quad \text{and} \quad B = \frac{\Delta H}{R} = 75,788 \tag{24}$$

Thus, P_{df} can be computed via Eqs. (19)–(24).

This model assumes that vapor can escape from powder source only when the diving force is greater than $\Delta P(r,z)$, the pressure barrier for vapor to escape from the powder. Since the pressure increases from the outer surface towards the center of the powder, powder near the crucible and crystal seed sublimes first. Therefore, reaction zones I and II, propagate from the outer surface of the powder to the center and their sizes are controlled by the driving

force, porosity and permeability of the powder, and reaction rate (see Fig. 1a).

To obtain the solution, the formulation describing the sublimation rate of reaction Eq. (9), is needed. Given by the Arrhenius relation, the sublimation rate can be expressed as [10]

$$\dot{R} = Z\frac{\exp\left(\frac{\Delta S}{R} - \frac{\Delta H}{RT}\right)}{P^{1.5}T^{1.2}}\frac{\Delta T}{L_d} \tag{25}$$

where $Z = 407.54$ is the pre-exponential factor determined from the experimental data [10], ΔT is the temperature difference between the source and seed. P is the pressure, and L_d is the distance between source and seed.

According to the mechanism of powder sublimation and porosity evolution, a central hole (Fig. 1b) is created in the powder such that vapor generated during sublimation can escape from both outer and inner surfaces of the powder. As a consequence, the reaction zone size can be increased and the sublimation rate is increased, which has also been adopted and proved by the experimental study.

6. Results and discussion

Basic thermophysical properties used in the simulation are taken from Refs. [11,17] and summarized in Table 1. The reaction zone thickness is defined as the length from the powder side surface to a location where 10% of powder is sublimed at a common axial coordinate $H/2$. The thickness represents the reaction zone size, as well as the sublimation rate. The history of the reaction zone thickness, the total sublimed AlN mass for powder with different initial porosities, particles sizes and driving forces are presented. In addition, the sublimed AlN mass is normalized to the maximum possible, e.g., the initial amount of AlN powder without porosity.

Table 1
Thermophysical properties used in the simulations

Properties	AlN	N_2 (at 2000 °C, 1 atm)
Specific heat (J/kg K)	1080	1297
Density (kg/m^3)	2500	0.1502
Thermal conductivity (W/m K)	220	0.1859
Viscosity (kg/m s)	–	642.6×10^{-7}
Kinematic viscosity (m^2/s)	–	427.8×10^{-6}

The electromagnetic field distribution in the entire furnace is shown in Fig. 2. The steady state temperature distribution in the furnace, the powder with and without a central hole is shown in Fig. 3. The highest temperature occurs at the lower part of the powder, which is related to the coil position of induction heating. Since the direction of heat transfer is from the crucible to the powder, temperature is higher at the crucible wall than at the center of the powder. Thus a higher reaction rate is achieved near the crucible wall.

To understand key transport phenomena, case studies are presented here. First, the effect of a central hole in the powder charge on the powder sublimation rate is studied. Fig. 4 shows the comparison of porosity distribution of AlN powder without a hole and with a central hole having different diameters: 1.0 cm and 1.6 cm. The initial porosity is set to be 0.2 and the sublimation time is 10 h. It is seen that AlN powder evaporates from the side surface of the hole, the outer and top surfaces of the powder. The pressure barrier $\Delta P(r,z)$ decreases when the hole is present, making vapor escape easier. Therefore, the reaction zone size and the sublimation rate are increased. Consequently, crystal growth rate will be increased. The total

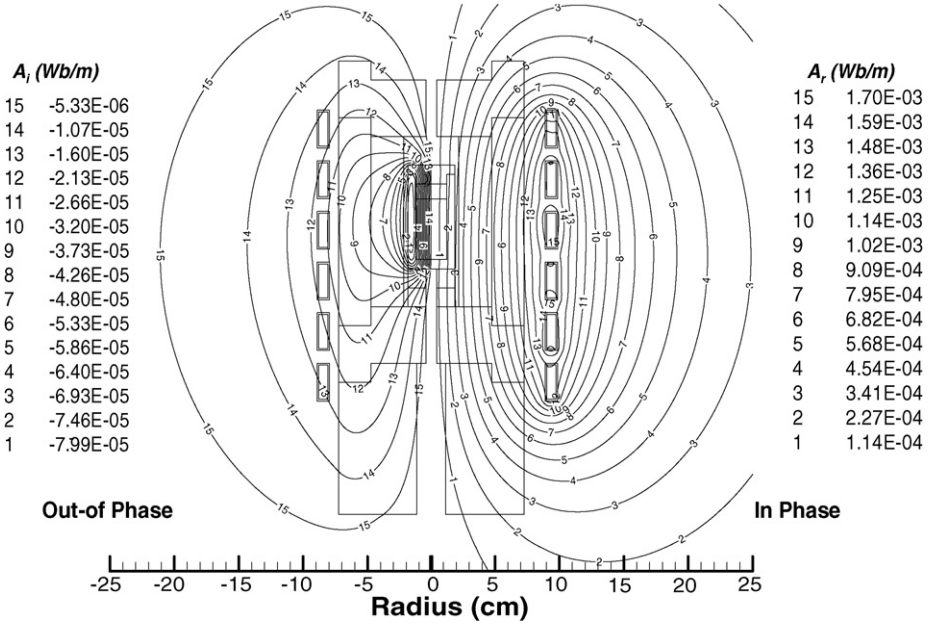

Fig. 2. Electromagnetic field distribution.

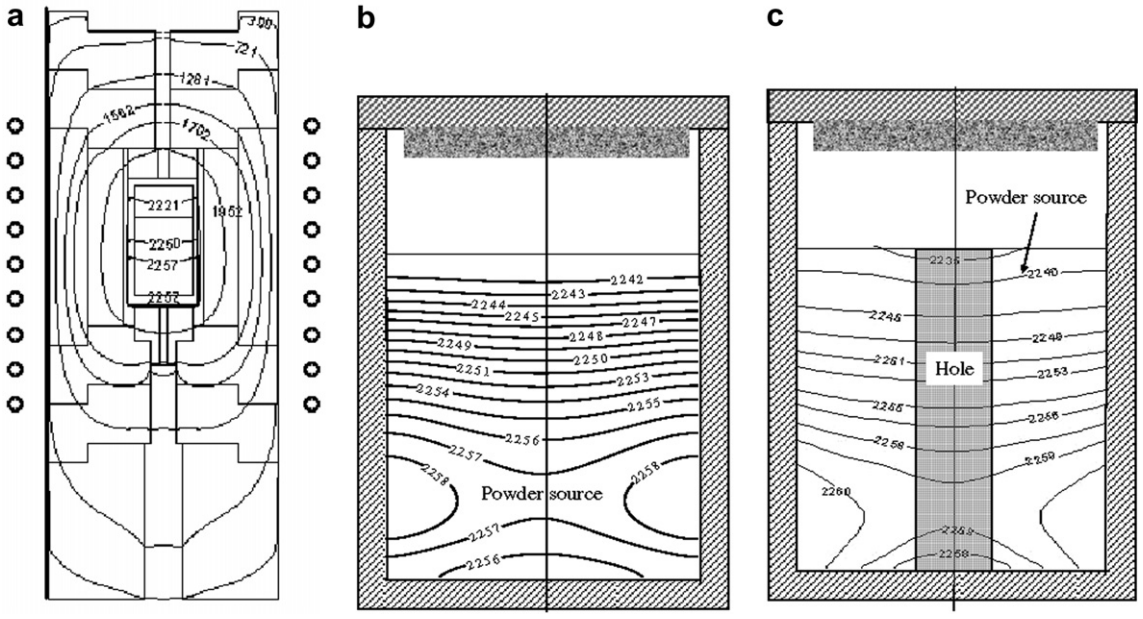

Fig. 3. Predicted temperature distributions (a) in the entire furnace (°C), (b) in the growth cell with the packed powder (°C), and (c) in the growth cell with a hole in the packed powder (°C).

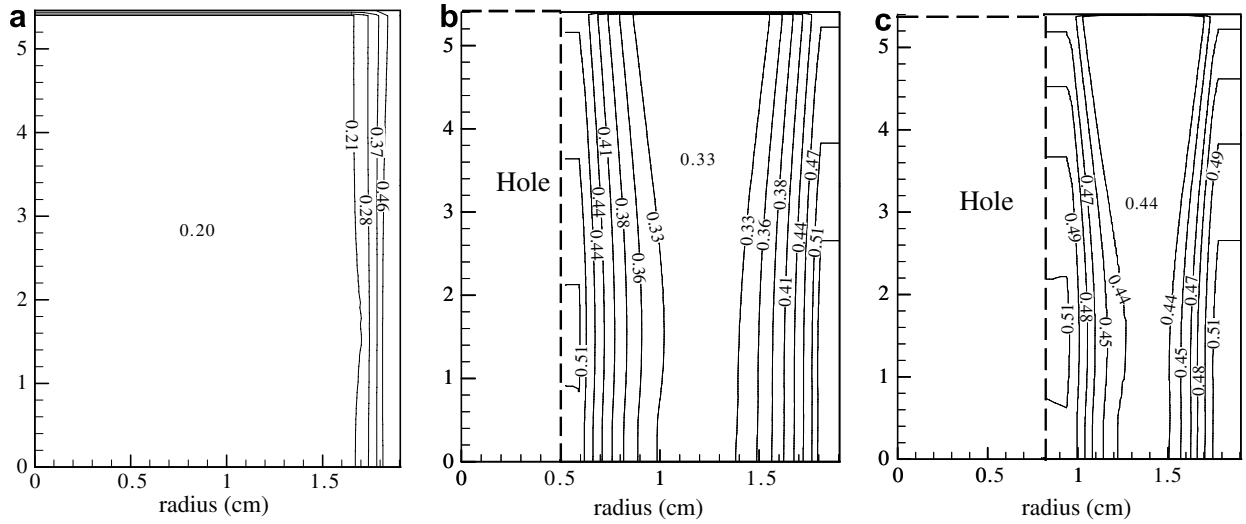

Fig. 4. Comparison of AlN porosity distribution without hole and with a central hole for different hole sizes, with initial porosity of 0.2 and sublimation time of 10 h: (a) no hole, (b) hole diameter of 1.0 cm, and (c) hole diameter of 1.6 cm.

and normalized sublimed AlN powder mass is presented in Fig. 5. After 30 h, the sublimed powder mass is increased by 80% and 85% for the powder with hole diameter of 1.0 cm and 1.6 cm, respectively. The experiments have also been performed for both cases with and without hole, and results show that the growth rate is increased by about 30% [18]. The discrepancy between the experimental and numerical results may be explained by crucible leakage. It is concluded that the powder sublimation rate remains the highest when the diameter of the hole is 1.6 cm for the first 10 h according to Fig. 5. However, the total mass of the initial powder decreases by increasing the initial size of the hole, which results in a decreased crystal size. In summary, both sublimation rate and total crystal size should be accounted for optimizing the sublimation process.

If surface reaction is assumed, e.g., the reaction rate is very fast and the permeability is low, the reaction area ratio and total mass ratio for powder with a central hole and without hole can be estimated as

$$\alpha = \frac{\pi DH + \pi dH + \pi(D^2 - d^2)/4}{\pi DH + \pi D^2/4} \tag{26}$$

$$\beta = \frac{\pi(D^2 - d^2)H}{\pi D^2 H} \tag{27}$$

where d is hole diameter. Using $D = 3.8$ cm and $H = 5.4$ cm, α and β are plotted as a function of $d(d < H/2)$,

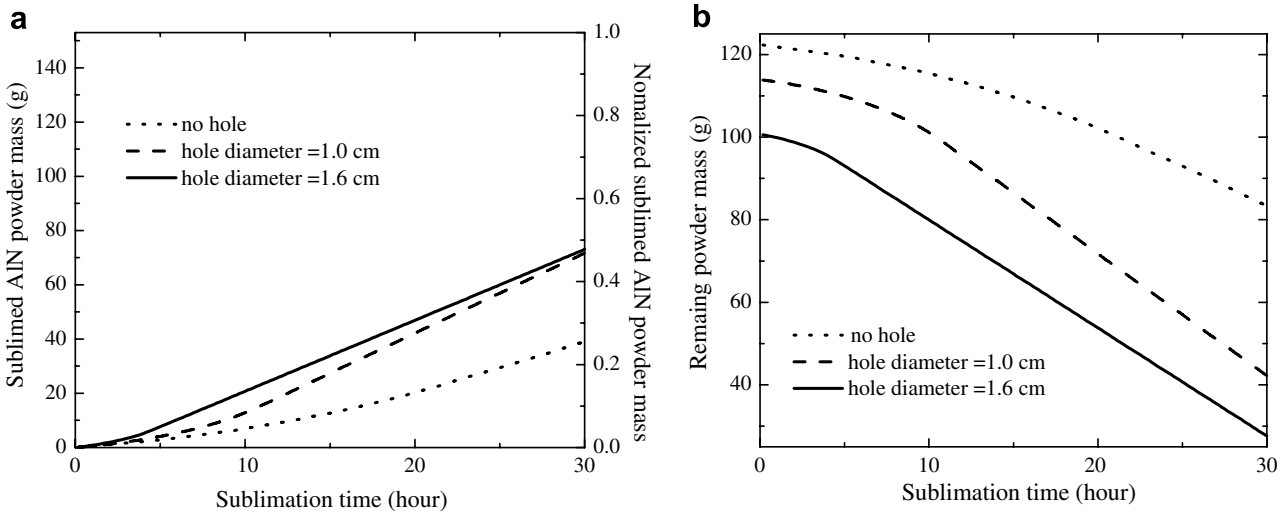

Fig. 5. Comparison of (a) sublimed AlN powder mass without hole and with one central hole and (b) remaining AlN powder mass.

as shown in Fig. 6. The reaction area increases as d increases, however, the total powder mass decreases. Considering both α and β, the optimal diameter of the hole is between 0.8 cm and 1.6 cm, as shown in the shaded area.

Second, the effect of initial powder porosity on the growth rate is investigated. Fig. 7 shows the comparison of the reaction zone thickness for powder with initial porosities of 0.18, 0.20, 0.22, 0.25 and 0.30, respectively. The simulation results show that the reaction zone thickness depends strongly on powder porosity. A slight increase in the porosity will result in large increase in the reaction zone thickness. Fig. 8 shows the comparison of both sublimed and remaining AlN powder mass. The sublimation rate is the highest for powder with an initial porosity of 0.3 in the first 20 h, and decreases after 20 h due to less availability of remaining powder. Therefore, a large system is needed to maintain high sublimation rate. It is concluded that the initial porosity between 0.25 and 0.3 is favorable since they show the pronounced enhancement in total gasification rate compared with the powder with initial porosity 0.18.

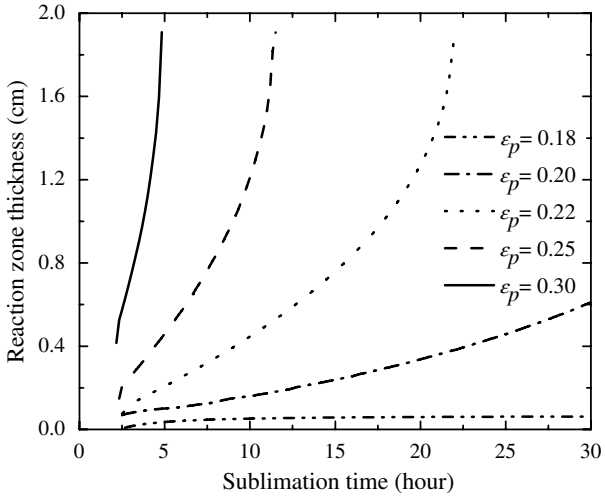

Fig. 7. Comparison of reaction zone thickness for powder with different initial porosities. The particle diameter is 0.02 cm.

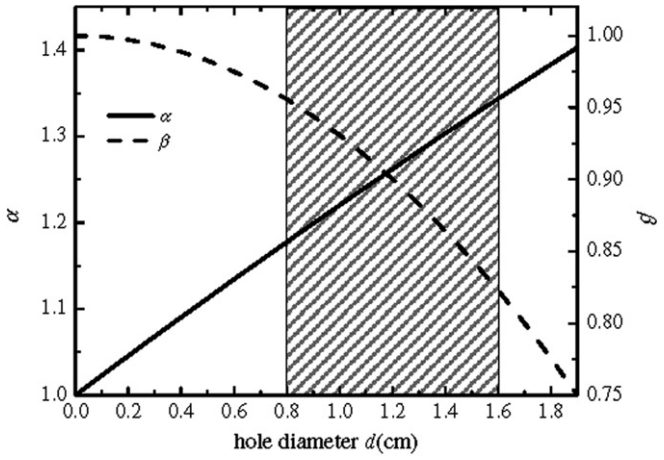

Fig. 6. Variation of α and β as a function of the hole diameter d.

Third, the effect of particle size on the growth rate is investigated. Fig. 9 shows the comparison of the reaction zone thickness for particles with diameters of 0.001, 0.005, 0.01, 0.015, 0.02 and 0.025 cm, respectively. The reaction zone thickness is the highest for the powder with the particle diameter of 0.025 cm. It is revealed that the reaction zone thickness also depends strongly on the particle size, although the influence of particle size on the reaction zone thickness is not as strong as that of the porosity by comparing Fig. 7 with Fig. 9. Fig. 10 shows the comparison of the sublimed AlN powder mass. It is concluded that the powder sublimation rate increases as the particle size increases. The reaction zone thickness and sublimed powder mass are the same for particles with diameter of

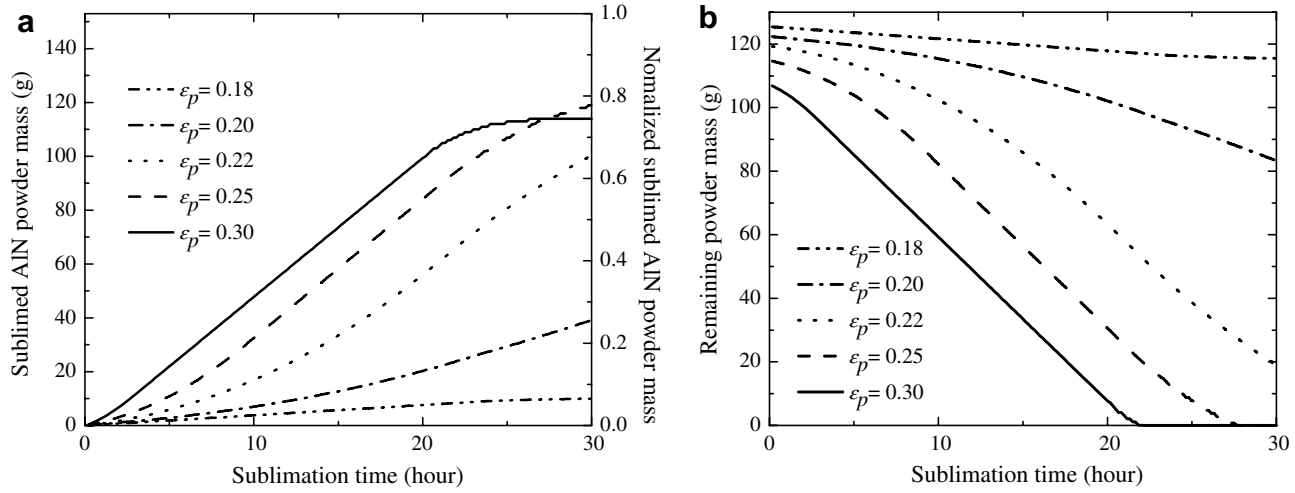

Fig. 8. Comparison of (a) sublimed AlN powder mass for different initial porosities and (b) remaining AlN powder mass. The particle diameter is 0.02 cm.

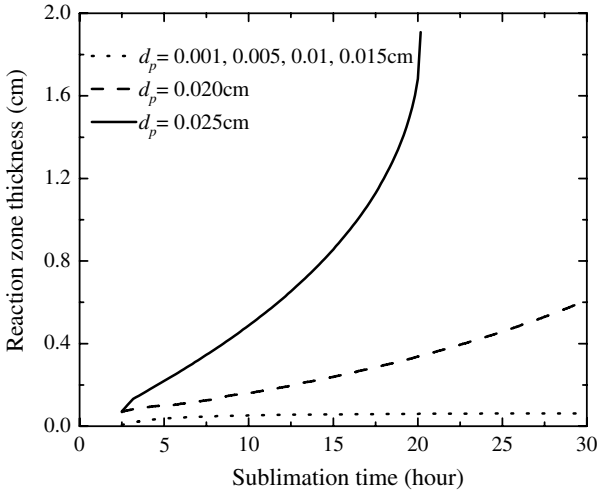

Fig. 9. Comparison of reaction thickness for powder with different particle sizes. The initial powder porosity is 0.2.

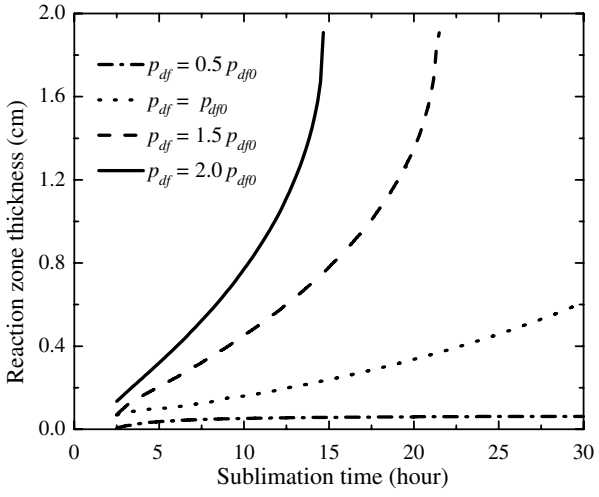

Fig. 11. Comparison of reaction thickness for different driving forces. The initial powder porosity is 0.2 and particle diameter is 0.02 cm.

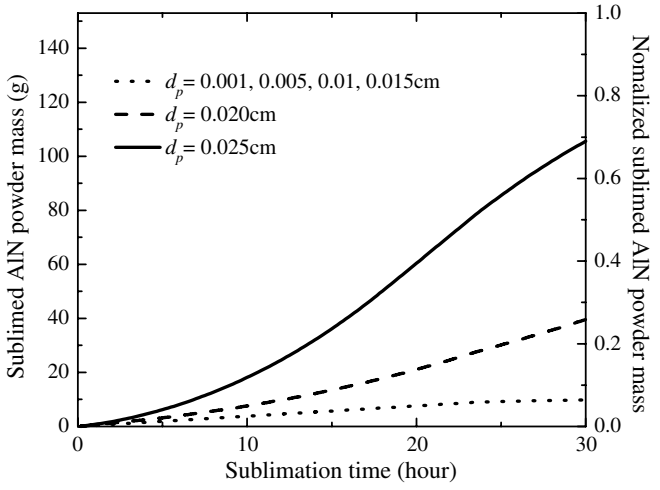

Fig. 10. Comparison of sublimed AlN powder mass for different particle sizes. The initial powder porosity is 0.2.

0.001, 0.005, 0.01, and 0.015 cm; it is due to the fact that the surface reaction is dominant in these cases.

Last, the effect of driving force on the growth rate is investigated. Fig. 11 shows the comparison of the reaction zone thickness for the diving forces of $0.5p_{df0}$,$1.0p_{df0}$,$1.5p_{df0}$ and $2.0p_{df0}$ respectively. It is concluded that the reaction zone thickness also depends on the driving force. A higher driving force results in a larger reaction zone. The influence of driving force on the reaction zone thickness is, however, weaker than porosity or particle size when comparing Fig. 11 with Fig. 7 and Fig. 11 with Fig. 9. Fig. 12 shows the comparison of the sublimed AlN powder mass. The powder sublimation rate increases as the driving force increases.

The reaction zone thickness l_{th} is determined by $\Delta P(r,z)$ and the diving force, and can be expressed analytically as a function of porosity, particle size, driving force, reaction rate, and time. Based on simulations, l_{th} can be formulated by interpolation as

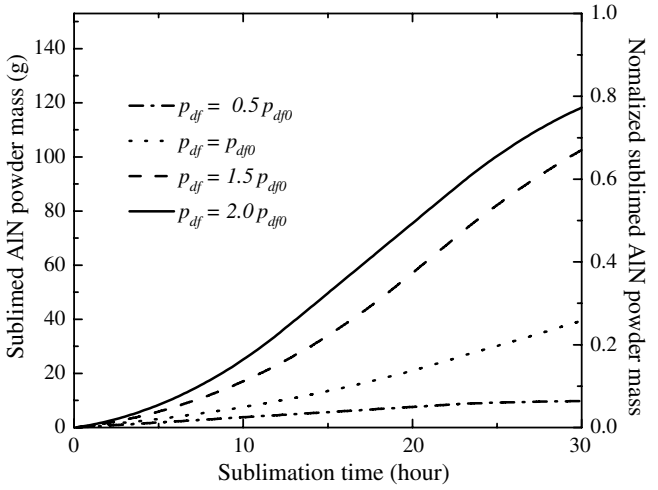

Fig. 12. Comparison of sublimed AlN powder mass for different driving forces. The initial powder porosity is 0.2 and particle diameter is 0.02 cm.

$$l_{\mathrm{th}} = Z_{\mathrm{th}} \frac{d_{\mathrm{p}}^2 \varepsilon_{\mathrm{p}}^3}{(1-\varepsilon_{\mathrm{p}})^2} P_{\mathrm{df}}^{1.8} \dot{R} t^{1.48} \tag{28}$$

where Z_{th} is a constant.

Considering the influence of both initial porosity and hole size on the sublimation rate, it is concluded that the optimal initial porosity should be between 0.25 and 0.3, and optimal hole diameter is between 1.0 cm and 1.6 cm, e.g., about 1/3 of crucible diameter in order to increase AlN powder evaporation rate and crystal growth rate.

7. Conclusions

A process model combining heat transfer, powder sublimation, vapor transport, and powder porosity evolution is presented. The temperature distribution in the AlN powder is calculated. It is found that the highest temperature occurs at the lower part of the powder and is close to the crucible wall, and the sublimation is expected to be the highest there. The mechanism of vapor transport is described by introducing a driving force. A novel approach of creating a central hole in the packed powder is proposed in order to increase crystal growth rate. The effect of the central hole on the sublimation rate is investigated. The simulation results indicate that the growth rate can be increased significantly (80–85%). The effects of initial porosity, particle size and driving force on the sublimation rate are also studied. Based on numerical simulations, optimal geometry of powder is determined. Optimal initial porosity is between 0.25 and 0.3 and optimal hole diameter between 1.0 cm and 1.6 cm, e.g., about 1/3 of the crucible diameter. The finding of this investigation can also be applied to SiC since SiC sublimation growth is similar to AlN.

Acknowledgement

We would like to acknowledge the sponsorship from DOE Award (DE-FC07-05ID14673).

References

[1] C. Tacitus, The Histories and the Annals, Harvard University Press, Cambridge, 1937, p. 4 v.
[2] J.C. Rojo, L.J. Schowalter, R. Gaska, M. Shur, M.A. Khan, J. Yang, D.D. Doleske, Growth and characterization of epitaxial layers on aluminum nitride substrates prepared from bulk, single crystals, J. Cryst. Growth 240 (2002) 508–512.
[3] D.F. Bliss, V.L. Tassev, D. Weyburne, J.S. Bailey, Aluminum nitride substrate growth by halide vapor transport epitaxy, J. Cryst. Growth 250 (1) (2003) 1–6.
[4] C.D. Blasi, Physico-chemical process occurring inside a degrading two-dimensional anisotropic porous medium, Int. J. Heat Mass Transfer 41 (1998) 4139–4150.
[5] G.Y. Meng, N. Azema, B. Cros, J. Durand, L. Cot, The growth mechanism of oriented AlN thin films by low-frequency plasma-enhanced metalorganic chemical vapour deposition process, J. Cryst. Growth 129 (3–4) (1993) 610–620.
[6] J.C. Rojo, G.A. Slack, K. Morgan, B. Raghothamachar, M. Dudley, L.J. Schowalter, Report on the growth of bulk aluminum nitride and subsequent substrate preparation, J. Cryst. Growth 231 (3) (2001) 317–321.
[7] N.B. Singh, A. Berghmans, H. Zhang, T. Wait, R.C. Clarke, J. Zingaro, J.C. Golombeck, Physical vapor transport growth of large AlN crystals, J. Cryst. Growth 250 (1–2) (2003) 107–112.
[8] R. Schlesser, Z. Sitar, Growth of bulk AlN crystals by vaporization of aluminum in a nitrogen atmosphere, J. Cryst. Growth 234 (2–3) (2002) 349–353.
[9] R. Schlesser, R. Dalmau, Z. Sitar, Seeded growth of AlN bulk single crystals by sublimation, J. Cryst. Growth 241 (4) (2002) 416–420.
[10] B. Wu, H. Zhang, Transport phenomena in an aluminum nitride induction heating sublimation growth system, Int. J. Heat Mass Transfer 47 (2004) 2989–3001.
[11] H. Zhang, B. Wu, D. Cai, L. Zheng, D.F. Bliss, V.L. Tessav, Group III nitride vapor growth systems: modeling and experiments, in: G.V. Karas (Ed.), Focus on Crystal Growth Research, Nova Science Pub Inc., New York, 2005, pp. 49–110.
[12] R.-H. Ma, H. Zhang, V. Prasad, M. Dudley, Growth kinetics and thermal stress in the sublimation growth of silicon carbide, Cryst. Growth Des. 2 (3) (2002) 213–220.
[13] R.-H. Ma, H. Zhang, S. Ha, M. Skowronski, Integrated process modeling and experimental validation of silicon carbide sublimation growth, J. Cryst. Growth 252 (2003) 523–537.
[14] M.F. Modest, Radiative Heat Transfer, McGraw-Hill, New York, 1993.
[15] R.G. Gann, Jr.R.H. Harris, J.F. Krasny, R.S. Levine, H.E. Mitler, T.J. Ohlemiller, The effect of cigarette characteristics on the ignition of soft furnishings, 1988.
[16] M.W. Chase, NIST-JANAF Thermochemical Tables, 4th ed., J. Phys. Chem. Ref. Data Monograph 9, American Chemical Society and American Institute of Physics, 1998.
[17] B. Wu, H. Zhang, Isotropic and anisotropic growth models for the sublimation vapour process, Model. Simulat. Mater. Sci. Eng. 13 (2005) 861–873.
[18] Personal communication with Drs. Z. Sitar and D.J. Zhuang in Department of Materials Science in North Carolina State University.